DALTON
FULL PAPER

Syntheses and reactions of some cluster complexes containing C_4 ligands with iron, ruthenium and cobalt carbonyls

Michael I. Bruce,*[a] Paul J. Low,[a] Natasha N. Zaitseva,[a] Samia Kahlal,[b] Jean-François Halet,*[b] Brian W. Skelton[c] and Allan H. White[c]

[a] *Department of Chemistry, University of Adelaide, Adelaide, South Australia 5005, Australia. E-mail: michael.bruce@adelaide.edu.au*
[b] *Laboratoire de Chimie du Solide et Inorganique Moléculaire, UMR CNRS 6511, Université de Rennes 1, 35042 Rennes Cedex, France*
[c] *Department of Chemistry, University of Western Australia, Nedlands, Western Australia 6907, Australia*

Received 27th March 2000, Accepted 28th June 2000
Published on the Web 9th August 2000

Some reactions of $W(C{\equiv}CC{\equiv}CH)(CO)_3Cp$ with metal cluster carbonyls have been studied. With $Ru_3(CO)_{10}(NCMe)_2$ the initial product is $Ru_3\{\mu_3\text{-}HC_2C{\equiv}C[W(CO)_3Cp]\}(\mu\text{-}CO)(CO)_9$, which readily transforms into $Ru_3(\mu\text{-}H)\{\mu_3\text{-}C_2C{\equiv}C[W(CO)_3Cp]\}(CO)_9$. Similar chemistry is found with the dppm analogue: three interconverting isomers of $Ru_3(\mu\text{-}H)\{\mu_3\text{-}C_2C{\equiv}C[W(CO)_3Cp]\}(\mu\text{-dppm})(CO)_7$ can be detected in solution. Reactions of $Ru_3(\mu\text{-}H)\{\mu_3\text{-}C_2C{\equiv}C[W(CO)_3Cp]\}(CO)_9$ with $Ru_3(CO)_{12}$ afforded $\{Ru_3(\mu\text{-}H)(CO)_9\}(\mu_3\text{-}\eta^2\text{:}\mu_3\text{-}\eta^2\text{-}C_2C_2)\{Ru_2W(CO)_8Cp\}$, while $Fe_2(CO)_9$ gave an analogous product in which three of the ruthenium sites are partially occupied by a total of one or two iron atoms; with $Co_2(CO)_8$ the vinylidene cluster $\{CoRu_2(CO)_9\}(\mu_3\text{-}\eta^2\text{:}\mu_3\text{-}\eta^2\text{-}CCHC_2)\{CoRuW(CO)_8Cp\}$ was formed, the cluster-bound hydride transferring to the C_4 ligand. The molecular structures of five complexes have been determined by single-crystal X-ray studies. Theoretical calculations have rationalised the tendency for the formation of $\mu_3\text{-}\eta^2\text{-}C_2$ fragments in these C_4 clusters.

Introduction

Compounds containing metal centres bridged by carbon chains are currently attracting much interest on account of their potential novel material properties, as well as their inherent theoretical interest.[1] In derivatives of even-numbered carbon chains, the possibility of alternative electronic configurations, ranging from polyyne (**A**) through cumulenic (**B**) to carbynic (**C**), has been demonstrated.[2] Most of this work has been developed using C_2 bridges, although recently extension into C_4[3,4] and longer chains has been reported.[4–6]

$\{M\}(C{\equiv}C)_x\{M\}$ **A** $\quad \{M\}{=}(C{=}C)_x{=}\{M\}$ **B** $\quad \{M\}{\equiv}C(C{\equiv}C)_{x-1}C{\equiv}\{M\}$ **C**

Cluster-bound carbon chains are much less common. This is particularly true for the sub-set containing C_4 chains, which currently comprises the following complexes: $\{Co_3(CO)_9\}_2(\mu_3\text{-}\eta^1\text{:}\mu_3\text{-}\eta^1\text{-}CC{\equiv}CC)$[7] and several $P(OMe)_3$ derivatives,[8] $\{Co_2M(CO)_8Cp\}(\mu_3\text{-}\mu_3\text{:}\eta^1\text{-}\eta^1\text{-}CC{\equiv}CC)\{Co_2M'(CO)_8Cp\}$ (M = M′ = Mo or W; M = Mo, M′ = W),[9] $[\{Fe_3(CO)_9\}_2(\mu_3\text{-}\eta^2\text{:}\mu_3\text{-}\eta^2\text{-}C_2C_2)]^{2-}$,[10] $\{M_3(\mu\text{-}PPh_2)(CO)_9\}_2(\mu_3\text{-}\eta^2\text{:}\mu_3\text{-}\eta^2\text{-}C_2C_2)$ (M = Ru or Os),[11] $Os_3(\mu\text{-}H)(CO)_{10}\{\mu\text{-}\eta^1\text{-}C{\equiv}CC{\equiv}C[Re(NO)(PPh_3)Cp^*]\}$ and $Os_3(\mu\text{-}H)(CO)_9\{\mu_3\text{-}\eta^2\text{-}C_2C{\equiv}C[Re(NO)(PPh_3)Cp^*]\}$.[12] Of some interest is the variety of modes of bonding of the C_4 moiety to the cluster, extending from the $\mu\text{-}\eta^1$ mode through the $\mu_3\text{-}\eta^1$ (**D**) to the $\mu_3\text{-}\eta^2$ (**E**) modes. In particular, the latter two may be related to the polyyne and carbynic modes found in carbon bridges linking mononuclear metal centres shown above.

In addition, we recently described the synthesis of the complex $W(C{\equiv}CC{\equiv}CH)(CO)_3Cp$ **1** (Scheme 1)[13] and briefly

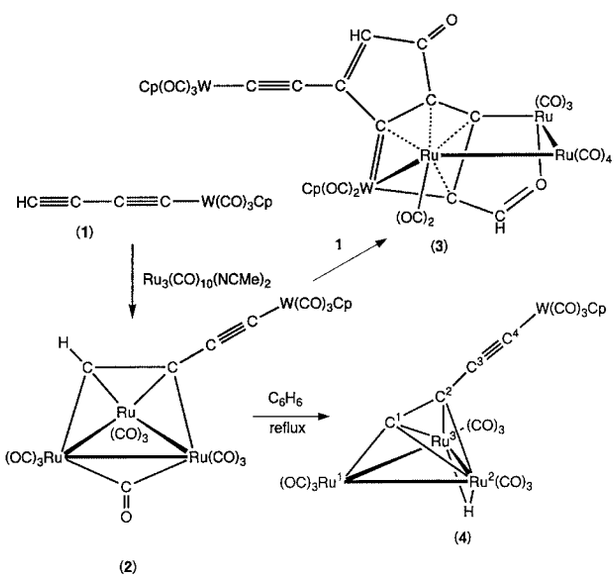

Scheme 1

reported its reaction with $Ru_3(CO)_{10}(NCMe)_2$ to give the expected μ_3-alkyne complex, $Ru_3\{\mu_3\text{-}\eta^2\text{-}HC_2C{\equiv}C[W(CO)_3Cp]\}(\mu\text{-}CO)(CO)_9$ **2**.[14] In turn, **2** reacts with a second molecule of **1** to give **3**, in which cyclisation with incorporation of CO involves the non-co-ordinated C≡C triple bond of **2**.[14] Complex **1** is a rich source of unusual complexes, including many containing the C_4 ligand; many of its reactions involve the C≡C triple bond furthest from the W atom. Herein we describe

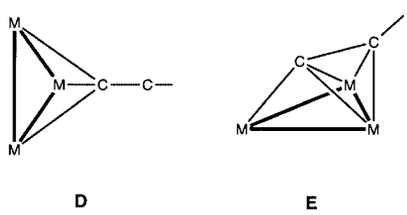

D **E**

DOI: 10.1039/b002406f

Table 1 Analytical and spectroscopic data

Complex	IR (CO)/cm^{-1}	NMR δ/J/Hz	ES MS m/z
2 $Ru_3\{\mu_3\text{-}HC_2C{\equiv}C[W(CO)_3Cp]\}(\mu\text{-}CO)(CO)_9$ Found: C, 27.33; H, 0.71. Calc. for $C_{22}H_6O_{13}Ru_3W$: C, 27.36; H, 0.62%	(cyclohexane): ν(C≡C) 2095w; ν(CO) 2063s, 2054vs, 2040m, 2028s, 2008m, 1962s, 1952s, 1928vw, 1914w, 1879w (br)	^{1}H: 5.61 (s, 5 H, Cp), 7.86 (s, 1 H, ≡CH)	(MeOH, negative ion): 883, $[M + H - 3CO]^-$; 855–743, $[M + H - nCO]^-$ (n = 4–8)
3 $Ru_3W\{\mu_4\text{-}OCHC_3C(O)CH{=}C(C{\equiv}C[W(CO)_3Cp])C\}(CO)_{11}Cp$ Found: C, 29.89; H, 0.82. Calc. for $C_{34}H_{12}O_{16}Ru_3W_2$: C, 30.29; H, 0.89%	(cyclohexane): ν(C≡C) 2093m; ν(CO) 2058s, 2039m, 2025s, 2018vs, 2014vs, 2005m, 1990m, 1962s, 1947s, 1921w, 1918w	^{1}H: 5.31 (s, 5 H, Cp), 5.55 (s, 1 H, CH), 5.67 (s, 5 H, Cp), 8.98 (s, 1 H, CHO)	(MeOH, positive ion): 1349, $[M + H]^+$; 1321, 1237, 1181, $[M + H - nCO]^+$ (n = 1, 4, 6)
4 $Ru_3(\mu\text{-}H)\{\mu_3\text{-}C_2C{\equiv}C[W(CO)_3Cp]\}(CO)_9$ Found: C, 26.89; H, 0.66. Calc. for $C_{21}H_6O_{12}Ru_3W$: C, 26.89; H, 0.64%	(cyclohexane): ν(C≡C) 2095w; ν(CO) 2070s, 2052s, 2043m, 2020vs, 1994 (sh), 1987w, 1966m, 1957m, 1943w, 1933vw	^{1}H: −20.33 (s, 1 H, RuH), 5.62 (s, 5 H, Cp)	(MeOH, negative ion): 911, $[M + H - CO]^-$; 883–743, $[M + H - nCO]^-$ (n = 2–7)
5 $Ru_3(\mu\text{-}H)\{\mu_3\text{-}\eta^1\text{:}\eta^2\text{-}C_2C{\equiv}C[W(CO)_3Cp]\}(\mu\text{-dppm})(CO)_7$ Found: C, 41.62; H, 2.26. Calc. for $C_{44}H_{28}O_{10}P_2Ru_3W$: C, 41.72; H, 2.21%	(CH_3Cl_2); ν(CO) 2062m, 2054m, 2037s, 2004vs, 1981s, 1948vs	^{1}H: −19.74 (t, J_{HP} = 15, 1 H, μ-H[2]), −19.21 (m, 2 H, μ-H[1]), 7.63–7.10 (m, 60 H, Ph), 3.17, 4.39 (2 × dt, J_{HH} = 12, J_{HP} = 12, 2 × 1 H, CH_2P_2[2]), 3.53, 4.39 (2 × dt, J_{HH} = 13, J_{HP} = 11, 2 × 2 H, CH_2P_2[1]), 5.50 (s, 5 H, Cp[2]), 5.65 (s, 10 H, Cp[1]) ^{13}C: 49.51 (t, J_{CP} = 25, CH_2P_2), 72.18 (s, C_α), 74.31 (s, C_β), 91.81 (s, Cp), 123.88 (s, Cγ), 132.54–127.88 (m, Ph), 152.17 (s, C_δ), 211.06 (s, CO), 229.07 (s, CO)	(MeOH containing NaOMe; positive ion): 1289, $[M + Na]^+$; 1261, $[M + Na - CO]^+$ (negative ion): 1297, $[M + OMe]^-$; 1265, $[M - H]^-$
6 $\{Ru_3(\mu\text{-}H)(CO)_9\}$ $(\mu_3\text{:}\mu_3\text{-}C_4)\{Ru_2W(CO)_8Cp\}$ Found: C, 24.84; H, 0.56. Calc. for $C_{26}H_6O_{17}Ru_5$: C, 24.39; H, 0.46%	(cyclohexane): ν(CO) 2074vs, 2069s, 2056s, 2035s, 2028s, 2010s, 1996m, 1987vw, 1975vw, 1964w, 1943w, 1935vw	^{1}H: −20.37 (s, 1 H, RuH), 5.57 (s, 5 H, Cp)	(MeOH, negative ion): 1226, $[M + H - 2CO]^-$; 1198–946, $[M + H - nCO]^-$ (n = 3–12)
7 $\{Ru_3(\mu\text{-}H)(CO)_9\}(\mu_3\text{:}\mu_3\text{-}C_4)\{RuFeW(CO)_8Cp\}$ Found: C, 26.23; H, 0.50. Calc. for $C_{26}H_6FeO_{17}Ru_4W$: C, 25.28; H, 0.49%	(cyclohexane): ν(CO) 2075vs, 2066s, 2055m, 2041m, 2026s, 2007s, 1992m, 1960m, 1951m	^{1}H: −20.39 (s, 1 H, RuH), 5.58 (s, 5 H, Cp)	(MeOH, negative ion): 1236, M^-; 1208–928, $[M - nCO]^-$ (n = 1–10)
8 $\{CoRu_2(CO)_9\}(\mu_3\text{-}\eta^2\text{:}\mu_3\text{-}\eta^2\text{-}CCHC_2)\{CoRuW(\mu\text{-}CO)(CO)_7Cp\}$ Found: C, 26.03; H, 0.51. Calc. for $C_{26}H_6Co_2O_{17}Ru_3W$: C, 26.11; H, 0.50%	(CH_2Cl_2): ν(CO) 2078m, 2058vw, 2047s, 2019s, 1959w (br), 1909w (br)	^{1}H: 5.59 (s, 5 H, Cp), 5.77 (s, 1 H, CH)	(MeOH, negative ion); 1196, M^-; 1141–916, $[M - nCO]^-$ (n = 2–10)

the chemistry of **2** in more detail, together with some related studies.

Results

The reaction between equimolar amounts of complexes **1** and $Ru_3(CO)_{10}(NCMe)_2$, carried out in dichloromethane, afforded dark red $Ru_3\{\mu_3\text{-}HC_2C{\equiv}C[W(CO)_3Cp]\}(\mu\text{-}CO)(CO)_9$ **2** in 40% yield, readily identified from its IR ν(CO) spectrum (Table 1), which resembles those of other μ_3-alkyne complexes of this type superimposed upon the ν(CO) spectrum of **1**. Several bands in the terminal ν(CO) region are present together with a weak band at 1879 cm^{-1} from the single bridging CO ligand. In addition a weak band at 2095 cm^{-1} is assigned to the ν(C≡C) absorption from the non-co-ordinated C≡C triple bond. In the ^{1}H NMR spectrum two signals at δ 5.61 and 7.86 arise from the Cp and ≡CH protons, respectively. No M^+ ion was found in the electrospray (ES) mass spectrum, the highest mass ion corresponding to $[M + H - 3CO]^+$, which fragments by loss of up to five more CO groups. We have been unable to obtain X-ray quality crystals of **2**, but its subsequent chemistry is consistent with the structure shown in Scheme 1.

Complex **2** can readily be converted into the corresponding hydrido-alkynyl cluster by brief heating in refluxing benzene, when yellow $Ru_3(\mu\text{-}H)\{\mu_3\text{-}C_2C{\equiv}C[W(CO)_3Cp]\}(CO)_9$ (**4**) was isolated in 67% yield. In its IR spectrum a weak band at 2095 cm^{-1} indicates the presence of the unco-ordinated C≡C triple bond and several terminal ν(CO) absorptions are present at lower energies. The ^{1}H NMR spectrum contains the cluster-bonded H atom resonance at δ −20.33 together with the singlet for Cp protons at δ 5.62. In the ES mass spectrum a weak peak at m/z 911 is assigned to $[M + H - CO]^+$ and is accompanied by fragment ions formed by loss of up to six more CO ligands. The molecular structure of **4** was confirmed by a single-crystal X-ray study, as reported below.

The complex $Ru_3(\mu\text{-dppm})(CO)_{10}$ is known to react readily with alkynes; terminal alkynes often undergo intramolecular oxidative addition so readily that μ-hydrido-alkynyl complexes are obtained directly.[15] We have previously described reactions of this complex with 1,4-diynes such as PhC≡CC≡CPh.[16] The reaction between $Ru_3(\mu\text{-dppm})(CO)_{10}$ and 1.5 equivalents of **1** afforded $Ru_3(\mu\text{-}H)\{\mu_3\text{-}\eta^1\text{:}\eta^2\text{-}C_2C{\equiv}C[W(CO)_3Cp]\}(\mu\text{-dppm})(CO)_7$ **5** (Scheme 2) (92%). Again, while the IR spectrum is similar in the ν(CO) region to those of related complexes, it also contains the ν(CO) bands of the $W(CO)_3Cp$ group. The ES mass spectrum of **5** with NaOMe present contained both $[M + Na]^+$ and $[M + Na - CO]^+$ cations. In the negative ion spectrum both the methoxide adduct $[M + OMe]^-$ and the deprotonated anion $[M - H]^-$ were observed.

In solution at r.t. the NMR spectra show that this complex exists as an interconvertible mixture of isomers (*ca.* 2:1), the major component (**5a**) showing the usual "windscreen-wiper" motion found for cluster-bound acetylide ligands.[17] The ^{1}H NMR spectra of **5a** at various temperatures are essentially identical to the spectra of $Ru_3(\mu\text{-}H)(\mu_3\text{-}\eta^1\text{:}\eta^2\text{-}C{\equiv}C^tBu)(\mu\text{-dppm})(CO)_7$ recorded under similar conditions.[17] A triplet resonance in the hydride region (δ −19.74, J_{HP} = 15 Hz) is attributable to the minor isomer (**5b**) in which the ^{31}P nuclei are equivalent.

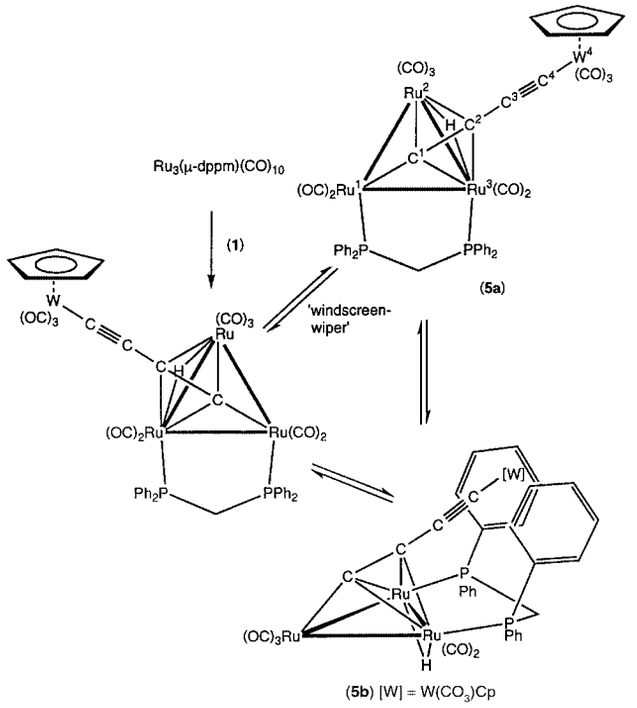

Scheme 2

Thus the μ-H ligand and μ-diynyl ligands must be bridging the Ru–Ru bond also bridged by the dppm ligand. The diynyl group in **5b** therefore lies between the phenyl rings of the dppm ligand in a manner similar to that found crystallographically in $Ru_3(\mu\text{-}H)(\mu_3\text{-}\eta^1\text{:}\eta^2\text{-}C_2C{\equiv}CSiMe_3)(\mu\text{-dppm})_2(CO)_5$.[18] There was no significant change in this signal upon lowering the temperature to 193 K. At temperatures above 313 K the hydride resonances began to collapse, and at 333 K the resonances from the hydride ligands of **5a** and **5b** had coalesced into a single broad signal, indicating rapid interconversion of all isomers. The results are summarised in Scheme 2. The solid-state structure of **5**, determined crystallographically (see below), corresponds to that of the major isomer (**5a**) observed in solution.

We have been interested in making complexes in which all four carbon atoms of a C_4 ligand are co-ordinated to the metal cluster core. In attempting to achieve this objective we have examined the reactions of **4** with several metal carbonyls (Scheme 3). On heating **4** with an equivalent amount of $Ru_3(CO)_{12}$ in refluxing toluene for 30 min, yellow-orange crystals of a new complex, identified as $\{Ru_3(\mu\text{-}H)(CO)_9\}(\mu_3\text{-}\eta^2\text{:}\mu_3\text{-}\eta^2\text{-}C_2C_2)\{Ru_2W(CO)_8Cp\}$ **6** by a single-crystal structure determination, were isolated in 53% yield. The spectroscopic properties of **6** were in accord with its solid-state structure, only terminal ν(CO) bands being seen in its IR spectrum between 2074 and 1935 cm^{-1}. The cluster-bound H atom and the Cp group give rise to singlet resonances at δ −20.37 and 5.57, respectively, in the ^{1}H NMR spectrum, while the ES mass spectrum contained ions between *m*/*z* 1226 and 946, corresponding to $[M + H - nCO]^+$ (n = 2–12).

A similar reaction between **4** and $Fe_2(CO)_9$ afforded an orange-red complex of idealised formula $\{Ru_{3-m}Fe_m(\mu\text{-}H)(CO)_9\}(\mu_3\text{-}\eta^2\text{:}\mu_3\text{-}\eta^2\text{-}C_2C_2)\{Ru_{2-n}Fe_nW(CO)_8Cp\}$ **7**, although X-ray structural studies showed that considerable disorder between Fe and Ru atoms was present. Careful separation by extensive t.l.c. gave three close-running fractions (orange-red, red and brown-red). Single crystals obtained from the first two fractions (**7a** and **7b**) had similar (disordered) structures, with $m + n = 1$ for **7a**, while for **7b**, $m + n = 2$. The major fraction had only terminal carbonyl ν(CO) absorptions with a pattern similar to that found for **6**. The ^{1}H NMR spectrum contained resonances at δ −20.39 and 5.58 for the Ru–H and Cp protons, respectively. The negative ion ES mass spectrum contained M^- at *m*/*z* 1236, corresponding to $m + n = 1$, and the fragment ions $[M - nCO]^-$ (n = 1–10).

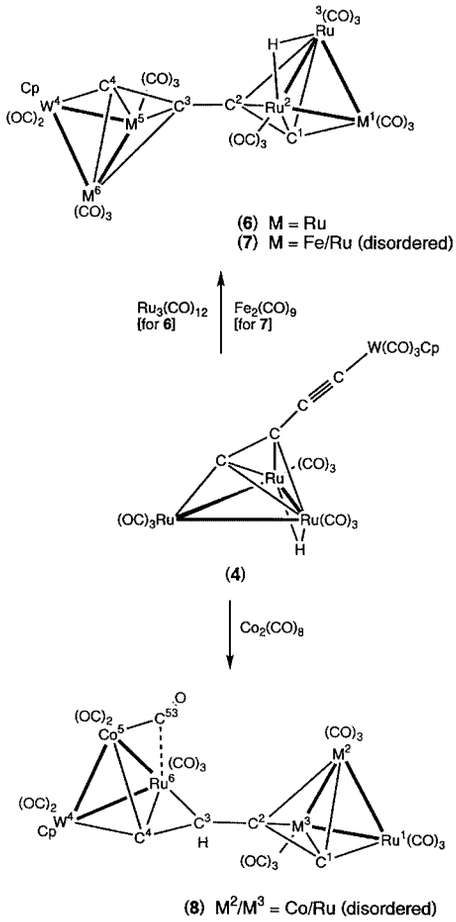

Scheme 3

The reaction between complex **4** and $Co_2(CO)_8$ was carried out in refluxing toluene for 15 min. The major product, isolated in 63% yield, was identified as $\{CoRu_2(CO)_9\}(\mu_3\text{-}\eta^2\text{:}\mu_3\text{-}\eta^2\text{-}CCHC_2)\{CoRuW(\mu\text{-}CO)(CO)_7Cp\}$ **8** from the X-ray study. In agreement with this formulation, the negative-ion ES mass spectrum contains M^- at *m*/*z* 1196, which loses up to 10 CO ligands. The IR spectrum contains five terminal ν(CO) bands between 2078 and 1959 cm^{-1}, together with a weak absorption at 1909 cm^{-1} which arises from the asymmetric μ-CO ligand. The ^{1}H NMR spectrum contains singlet resonances at δ 5.59 and 5.77 with relative intensities 5:1; no high-field signal is present. The single proton resonance can be assigned to the vinylidene proton H(3) found in the structural study.

Molecular structures of complexes 4–8

Plots of single molecules of **4**, **5a**, **6** and **8** are given in Figs. 1–4 (complexes **7** being isomorphous with **6**), while structural parameters are collected in Tables 2 and 3. Descriptions of each will be given separately.

(a) $Ru_3(\mu\text{-}H)\{\mu_3\text{-}C_2C{\equiv}C[W(CO)_3Cp]\}(CO)_9$ 4. The structure of complex **4** is similar to those of several other hydrido-alkynyl clusters of ruthenium, with the ethynyl group attached in μ_3 fashion to a closed triangular Ru_3 cluster [Ru–Ru 2.7934(7)–2.8006(5) Å], with the hydride located across the Ru(2)–Ru(3) vector. The Ru(1)–C(1) distance is 1.955(4) Å, consistent with an Ru–C σ bond, while C(1,2) are π bonded to the other two Ru atoms [Ru(2,3)–C(1,2) 2.204(5)–2.283(6) Å], distances to C(2) being appreciably longer than to C(1). The C(1)–C(2) separation is 1.327(5) Å. The substituent on C(2) is the $C{\equiv}CW(CO)_3Cp$ group, with C(2)–C(3) 1.391(6), C(3)–C(4) 1.210(7) and

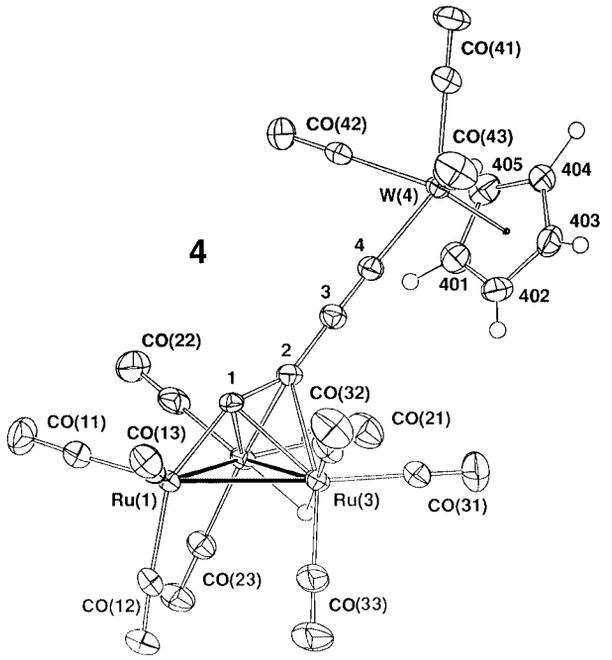

Fig. 1 Plot of a molecule of $Ru_3(\mu\text{-}H)\{\mu_3\text{-}C_2C{\equiv}C[W(CO)_3Cp]\}(CO)_9$ **4**, showing the atom numbering scheme. In this and subsequent figures, non-hydrogen atoms are shown with 20 (r.t.) or 50% (low temperature) 'thermal' envelopes; hydrogen atoms have arbitrary radii of 0.1 Å. Settings of the figures correspond to those in Scheme 3.

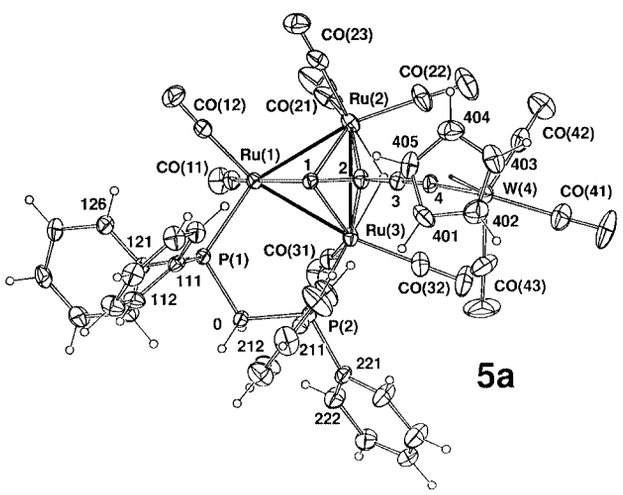

Fig. 2 Plot of a molecule of $Ru_3(\mu\text{-}H)\{\mu_3\text{-}C_2C{\equiv}C[W(CO)_3Cp]\}$-$(\mu\text{-dppm})(CO)_7$ **5**, showing the atom numbering scheme.

W–C(4) 2.136(5) Å. Other structural parameters for the $W(CO)_3Cp$ group fall within the range found for earlier reported examples.[13,19] Complexation of the C(1)–C(2) moiety to the Ru_3 cluster results in bending of the C(1)–C(2)–C(3) chain to 150.5(5)° and in the opposite direction, of Ru(1)–C(1)–C(2) to 153.7(4)° [τ{Ru(1)–C(1)–C(2)–C(3)} 179.8(8)°]. Angles at C(3) and C(4) are 173.5(6) and 175.2(5)°, respectively.

(b) $Ru_3(\mu\text{-}H)\{\mu_3\text{-}\eta^1:\eta^2\text{-}C_2C{\equiv}C[W(CO)_3Cp]\}(\mu\text{-dppm})(CO)_7$ 5a. In complex **5a** the dppm ligand has substituted one CO ligand on each of Ru(1) and Ru(2) of **4**, the molecular structure otherwise being essentially the same. The Ru–Ru distances range between 2.777(3) and 2.800(2) Å, the shortest being that bridged by the dppm ligand. The Ru–P distances are normal at 2.294 and 2.329(2) Å and the geometry of the dppm is similar to others reported earlier [P(1,2)–C(0) 1.833, 1.836(7) Å, Ru(*n*)–P(*n′*)–C(0) 112.4, 109.6(2), P(1)–C(0)–P(2) 111.2(4)°] (note: $n \neq n'$). The alkynyl group attached to the Ru_3 cluster is similar to that found in **4**, bond lengths and angles being identical within experimental error. The cluster-bound H atom was located bridging the Ru(2)–Ru(3) vector.

Table 2 Selected bond parameters (lengths in Å, angles in °) for complexes **4**, **5a** and **8**[a]

	4	**5a**	**8**
M(1)–M(2)	2.7990(8)	2.796(2)	2.764(1)
M(1)–M(3)	2.8006(5)	2.777(3)	2.710(2)
M(2)–M(3)	2.7934(7)	2.800(2)	2.568(2)
M(4)–M(5)			2.683(2)
M(4)–M(6)			2.978(2)
M(5)–M(6)			2.672(2)
M(1)–C(1)	1.955(4)	1.980(7)	1.94(1)
M(2)–C(1)	2.204(5)	2.223(7)	2.160(7)
M(2)–C(2)	2.277(5)	2.274(7)	2.210(9)
M(3)–C(1)	2.224(5)	2.200(6)	2.07(1)
M(3)–C(2)	2.283(6)	2.302(7)	2.200(9)
M(4)–C(4)	2.136(5)	2.134(7)	2.013(6)
M(5)–C(3)			—
M(5)–C(4)			1.936(9)
M(6)–C(3)			2.292(9)
M(6)–C(4)			2.163(9)
C(1)–C(2)	1.327(5)	1.318(9)	1.30(1)
C(2)–C(3)	1.391(6)	1.39(1)	1.46(1)
C(3)–C(4)	1.210(7)	1.19(1)	1.39(1)

For **5a**: M(1)–P(1) 2.294(2), M(3)–P(2) 2.329(2), P(1)–C(0) 1.833(7), P(2)–C(0) 1.836(7)

M(1)–C(1)–C(2)	153.7(4)	153.1(5)	155.8(6)
C(1)–C(2)–C(3)	150.5(5)	149.7(7)	150.1(7)
C(2)–C(3)–C(4)	173.5(6)	178.3(7)	124.4(7)
C(3)–C(4)–M(4)	175.2(5)	174.7(6)	148.9(7)
C(3)–C(4)–M(5)			119.8(5)

For **5**: M(1)–P(1)–C(0) 112.4(2), M(3)–P(2)–C(0) 109.6(2), P(1)–C(0)–P(2) 111.2(4)

[a] For complexes **4**, **5**, M(1–3) = Ru, M(4) = W; for **8**, M(1) = Ru, M(2,3,6) = Co, M(4) = 0.859(6) Co/[1 − 0.859(6)] Ru, M(5) = [1 − 0.859(6)] Co/0.859(6) Ru.

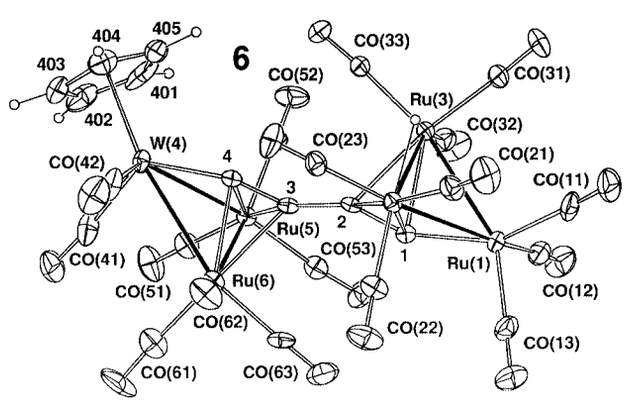

Fig. 3 Plot of a molecule of $\{Ru_3(\mu\text{-}H)(CO)_9\}(\mu_3{:}\mu_3\text{-}C_2C_2)\{Ru_2$-$W(CO)_8Cp\}$ **6**, showing the atom numbering scheme.

(c) $\{Ru_3(\mu\text{-}H)(CO)_9\}(\mu_3\text{-}\eta^2{:}\mu_3\text{-}\eta\text{-}C_2C_2)\{Ru_2W(CO)_8Cp\}$ 6. In this complex the C_4 ligand is found attached to each M_3 cluster in the $\mu_3\text{-}2\eta^1{:}\eta^2$ fashion found in **4** and **5**. The Ru_3 cluster can be compared directly with that found in **4**: a somewhat larger range of Ru–Ru distances [2.672–2.823(1) Å] is found, the average separation being *ca.* 0.01 Å longer in **6**. The cluster-bound H atom bridges the Ru(2)–Ru(3) bond. While the Ru(1)–C(1) σ bonds are the same in **4** and **6** [1.955(4) and 1.944(9) Å], the π bonds are somewhat shorter in the latter [2.197–2.210(9) Å].

Table 3 Variation in bond lengths (Å) and angles (°) with incorporation of Fe in complexes **6** and **7**

	7b(ii)	7b(i)	7a(i)	7a(ii)	6
Proportion of Ru at each site (x), Fe constrained to ($1 - x$)					
M(1)	0.257(5)	0.554(6)	0.694(8)	0.740(3)	100
M(5)	0.183(4)	0.083(6)	0.478(8)	0.407(3)	100
M(6)	0.478(4)	0.364(6)	0.860(8)	0.872(3)	100
Total Ru/Fe (%)	92/208	100/200	203/97	202/98	300/0
M(1)–Ru(2)	2.7789(8)	2.801(1)	2.809(1)	2.8173(5)	2.823(1)
M(1)–Ru(3)	2.7794(8)	2.803(1)	2.807(1)	2.8135(5)	2.819(1)
Ru(2)–Ru(3)	2.7837(7)	2.7876(9)	2.783(2)	2.7877(6)	2.785(2)
W(4)–M(5)	2.8777(7)	2.864(1)	2.906(1)	2.9066(5)	2.952(1)
W(4)–M(6)	2.9563(6)	2.9501(9)	2.983(1)	2.9867(5)	2.988(1)
M(5)–M(6)	2.5731(8)	2.547(1)	2.619(2)	2.6185(6)	2.672(1)
M(1)–C(1)	1.821(5)	1.855(7)	1.903(7)	1.898(4)	1.944(9)
Ru(2)–C(1)	2.188(5)	2.184(6)	2.221(9)	2.196(3)	2.205(8)
Ru(2)–C(2)	2.229(5)	2.227(6)	2.226(8)	2.234(3)	2.210(9)
Ru(3)–C(1)	2.192(5)	2.182(7)	2.209(9)	2.197(3)	2.197(9)
Ru(3)–C(2)	2.213(5)	2.211(6)	2.221(8)	2.219(3)	2.197(8)
W(4)–C(4)	1.985(5)	1.972(7)	1.966(7)	1.991(3)	1.975(9)
M(5)–C(3)	2.099(4)	2.072(6)	2.117(9)	2.126(3)	2.186(9)
M(5)–C(4)	2.078(4)	2.056(6)	2.111(9)	2.126(3)	2.208(8)
M(6)–C(3)	2.165(5)	2.143(7)	2.202(9)	2.206(3)	2.232(9)
M(6)–C(4)	2.125(5)	2.112(6)	2.174(9)	2.188(3)	2.181(8)
C(1)–C(2)	1.333(7)	1.33(1)	1.33(1)	1.329(5)	1.30(1)
C(2)–C(3)	1.410(7)	1.425(9)	1.40(1)	1.411(4)	1.43(1)
C(3)–C(4)	1.301(7)	1.31(1)	1.33(1)	1.312(5)	1.32(1)
M(1)–C(1)–C(2)	155.0(4)	155.7(6)	152.1(7)	154.3(3)	151.9(7)
C(1)–C(2)–C(3)	147.3(4)	147.7(6)	143.9(8)	146.3(3)	143.6(8)
C(2)–C(3)–C(4)	148.0(4)	147.7(6)	145.9(9)	146.4(3)	145.9(8)
C(3)–C(4)–W(4)	160.0(4)	159.8(5)	159.5(7)	158.4(3)	158.9(7)

The Ru(5)–Ru(6) bond in the Ru_2W cluster is much shorter [2.672(1) Å], consistent with there being no μ-H atom present; the two Ru–W separations are 2.952 and 2.988(1) Å. The attachment of C(3)–C(4) to this cluster is by a W–C(4) σ bond [1.975(9) Å] and by π bonds to Ru(5) and Ru(6) [Ru(5,6)–C(3,4) 2.181–2.232(9) Å]. The tungsten atom carries a Cp group and two CO ligands, with W–C separations similar to those found in **5**. Along the C_4 chain, angles at C(1–4) are 151.9, 143.6, 145.9 and 158.9(7)°.

(d) $\{Ru_{3-m}Fe_m(\mu\text{-}H)(CO)_9\}(\mu_3\text{-}\eta^2\text{:}\mu_3\text{-}\eta^2\text{-}C_2C_2)\{Ru_{2-n}Fe_n\text{-}W(CO)_8Cp\}$ 7. In complex **7**, partial substitution of ruthenium by iron is found at the M(1), M(5) and M(6) sites. Two samples of each of the two fractions (**7a**, **7b**) from two syntheses were examined structurally and, after trial refinement, refined in terms of a model in which a total of one (**7a**) or two (**7b**) ruthenium atoms have been replaced by iron. Table 3 compares the results for various samples of **7** with those of **6** and summarises the changes that occur as decreasing proportions (from 74 to 0%, *i.e.* **6**) of the smaller iron atom are incorporated. Percentage iron occupancies of the three sites M(1,5,6) range from 26, 52, 12 to 74, 92, 64%. This leads to a progressive shortening of bond distances involving these atoms, as expected. For example, M(5)–M(6) lie between 2.619(2) and 2.547(1) Å, shorter than Ru(5)–Ru(6) in **6** by between 0.05_3 and 0.12_5 Å, while W–M(5,6) are shortened by between 0.04_5 and 0.08_8 Å; curiously, the effect is more pronounced with M(5). In the Ru_3 cluster the Ru(2)–Ru(3) separations are identical in **6**, **7a** and **7b** (a useful indicator of internal consistency), but M(1)–Ru(2,3) bonds are shorter by between 0.04_4 and 0.01_5 Å. Larger changes are found in the M(6)–C(3,4) bonds, which are shortened to between 2.143(7) and 2.206(3) and 2.112(6) and 2.188(3) Å, respectively, from the values of 2.181, 2.232(9) Å found in **6**; the M(1)–C(1) σ bond changes from 1.944(9) (**6**) to between 1.903(7) and 1.821(5) Å. Comparison with $FeRu_2(CO)_{12}$,[20] which has Fe–Ru distances of 2.775 and 2.763(2) Å and an Ru–Ru separation of 2.8059(9) Å, *i.e.* a difference of *ca.* 0.037 Å, shows that clusters **7** exhibit considerably higher contractions of the M–M bonds upon replacement of Ru by Fe.

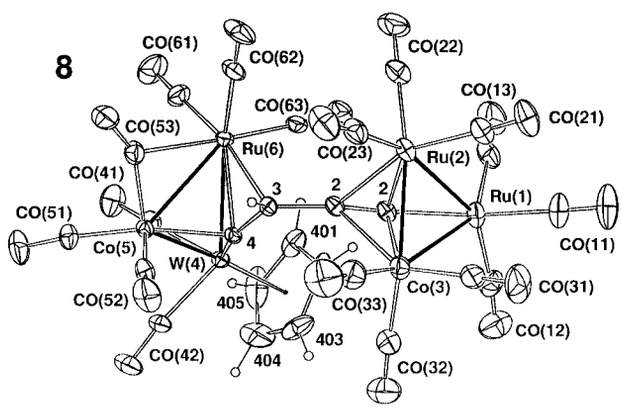

Fig. 4 Plot of a molecule of $Co_2Ru_3W(\mu_3\text{:}\mu_3\text{-}CCHC_2)(CO)_{17}Cp$ **8**, showing the atom numbering scheme.

In complexes **6** and **7** the attachment of the alkynyl groups to the tungsten-containing cluster is influenced by the position of the cyclopentadienyl group, which is to one side of the cluster. In **6**, for example, the alkynyl group is skewed across the cluster so that the Ru(5)–C(3,4) bonds (2.186(9), 2.208(8) Å) differ from the Ru(6)–C(3,4) bonds (2.232(9), 2 .181(8) Å).

(e) $\{CoRu_2(CO)_9\}(\mu_3\text{-}\eta^2\text{:}\mu_3\text{-}\eta^2\text{-}CCHC_2)\{CoRuW(\mu\text{-}CO)(CO)_7Cp\}$ 8. In complex **8** we find substitution of two Ru atoms by cobalt to give $CoRu_2$ (A) and CoRuW (B) clusters. In the former Co/Ru disorder is present in positions M(2) and M(3). A range of metal–metal bond distances is found, from 2.568(2) to 2.764(1) Å in the $CoRu_2$ cluster and from 2.672(2) to 2.978(2) Å in the CoRuW cluster. The shortest distances involve the Co atoms [M(2)–M(3) in cluster A; in cluster B, surprisingly, the Co(5)–Ru(6) separation is only 0.01_1 Å shorter than the Co(5)–

W(4) separation]. The only other example of a $CoRu_2$ cluster bearing a μ_3-alkynyl ligand, to our knowledge, is that present in $Co_2Ru_3(\mu_4\text{-}C_2Ph)(\mu_3\text{-}C_2Ph)(\mu\text{-dppm})(\mu\text{-CO})(CO)_9$, in which the analogous Co–Ru separations are 2.5583(9) and 2.751(1) Å, with the Ru–Ru bond, also bridged by the dppm ligand, being 2.850(2) Å.[21] In **8** the tungsten atom retains the Cp group and is additionally attached to two terminal CO groups. Atoms Ru(1,2), Co(3) carry three terminal CO groups each; however, in the CoRuW cluster, atoms Co(5) and Ru(6) have respectively two and three terminal CO groups, while the Co(5)–Ru(6) vector is bridged unsymmetrically by CO(53) [Co(5)–C(53) 1.80(1), Ru(6)–C(53) 2.35(1) Å; Co(5)–C(53)–O(53) 151(1), Ru(6)–C(53)–O(53) 130(1)°].

A hydrogen atom is present on C(3) of the carbon chain, the ligand thus formally being an alkynylvinylidene, with each half being attached to the respective clusters in different modes. The alkynyl portion is attached in the usual $\mu_3(\perp)$ fashion to the $CoRu_2$ cluster, atom C(1) being σ-bonded to Ru(1) [1.94(1) Å]. The C(1)–C(2) separation is 1.30(1) Å, with angles at C(1) and C(2) of 155.8(6) and 150.1(7)°, respectively. In the Co_2Ru_3 cluster mentioned above the Ru–C σ bond is 1.992(4) Å and the π bonds from the C_2 unit to Co and Ru are 2.117, 2.212(3) and 2.193, 2.257(4) Å, respectively. Angles at the two carbon atoms are 156.6(3) and 146.9(4)°.[21] The C(3)–C(4) moiety is attached to the CoRuW cluster by two σ bonds from C(4) to Co(5) and W(4) [1.936(9) and 2.013(6) Å, respectively] and by an asymmetric π bond from both carbons to Ru(6) [Ru–C(3,4) 2.292(9), 2.163(9) Å], as found in other cluster-bonded vinylidenes.[22] The angle C(2)–C(3)–C(4) is 124.4(7)°, consistent with an sp^2-hybridised carbon. The C(2)–C(3) and C(3)–C(4) separations are 1.46(1) and 1.39(1) Å, consistent with single and double bonds, respectively, the latter being lengthened by electron donation to Ru(6). In $Co_2Ru(\mu_3\text{-}CCHBu^t)(CO)_9$ the Co–C σ bonds are 1.901, 1.893(7) Å and the Ru–C bonds are 2.099(8) and 2.405(8) Å, somewhat smaller and larger, respectively, than those found in **8**.[23]

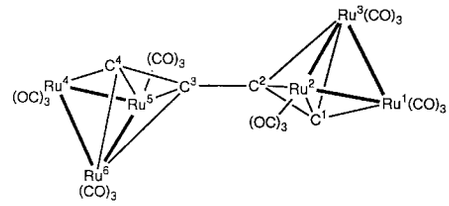

(9)

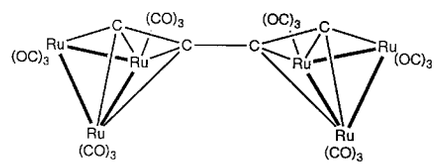

(10)

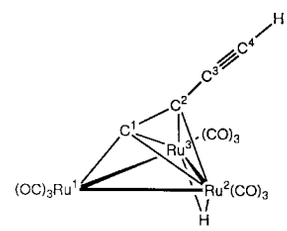

(11)

Theoretical considerations

With the $C_2C{\equiv}C\{W(CO)_3Cp\}$ moiety lying perpendicular to one metal–metal bond, cluster **4** can be considered as a trimetallic "acetylide" $M_3\{\mu_3(\perp)\text{-}C_2R\}$ complex. In terms of electron counting, $M_3\{\mu_3(\perp)\text{-}C_2R\}$ complexes are expected to have 48 cluster valence electrons (c.v.e.). This electron count is satisfied for **4** if the $C_2C{\equiv}C\{W(CO)_3Cp\}$ group serves as a 5-electron donor. A similar bonding mode is observed in species **6** and **7** in which two carbon atoms on each end of the non-linear C_4 chain are bound to a metallic triangle. Indeed, such compounds consist of two 48-c.v.e. trimetallic "acetylide" $M_3\{\mu_3(\perp)\text{-}C_2R\}$ clusters joined by a C–C single bond, with the diynyl moiety acting as a 10-electron donor. The same 48-c.v.e. trimetallic "acetylide" unit is present in compound **8** linked to a 48-c.v.e. trimetallic vinylidene $M_3\{(\mu_3(\perp)\text{-}CCHR\}$ cluster. These "classical" electron counts are obtained if the alkynylvinylidene ligand contributes 9 (5 + 4) electrons to the two cluster units.

Quantum chemical calculations of extended Hückel (EH) and density functional (DF) type were carried out on clusters **6** and **8** (see the Theoretical calculations section in the Experimental section) in order to provide a better insight into their electronic structures, in particular to see whether intracluster interaction occurs between the two metallic halves of the clusters through the unsaturated C_4 bridge. EH calculations were first carried out on the DF-optimised hypothetical homometallic dianion $[\{Ru_3(CO)_9\}_2(\mu_3\text{-}\eta^2\text{:}\mu_3\text{-}\eta^2\text{-}C_2C_2)]^{2-}$ **9**[24] in order to analyse qualitatively the bonding between the metallic and carbon moieties in this kind of cluster complex.

The qualitative MO diagram of the ruthenium model **9**, which is isostructural and isoelectronic to the observed iron species $[\{Fe_3(CO)_9\}_2(\mu_3\text{-}\eta^2\text{:}\mu_3\text{-}\eta^2\text{-}C_2C_2)]^{2-}$,[10] is shown in Fig. 5 and is based on the interaction of the frontier molecular orbitals (FMOs) of the $\{(CO)_9Ru_3\cdots Ru_3(CO)_9\}$ metallic framework with the FMOs of the $(C_4)^{2-}$ unit.[25]

The metallic fragment consists of two non-interacting $Ru_3(CO)_9$ triangular units. Typically, each metal triangle is made of three conical ML_3 groups giving rise to a nest of nine "t_{2g}" d-type levels below a low-lying set of three FMOs which extend predominantly in the metal plane and, at somewhat higher energy, a set of three orbitals extending mainly out of the metal plane.[26] Consequently, the $\{(CO)_9Ru_3\cdots Ru_3(CO)_9\}$ metallic framework of C_{2h} symmetry exhibits a set of six vacant out-of-plane FMOs ($2a_u$, $3a_g$, $3b_u$, $2b_g$, $4a_g$ and $4b_u$), somewhat separated in energy from a set of occupied in-plane FMOs ($1a_u$, $1b_g$, $1a_g$, $1b_u$, $2a_g$ and $2b_u$), lying above a "t_{2g}" block of eighteen orbitals (see the left-hand side of Fig. 5).

The MOs of the *trans*-bent $(|C{\equiv}CC{\equiv}C|)^{2-}$ unit (of C_{2h} symmetry) differ somewhat from those of a linear chain. Bending at the central C(2) and C(3) carbon atoms splits the initially degenerate π and π* orbital sets (see Fig. 6). The orbitals perpendicular to the bending plane do not change in energy upon bending, whereas those lying in the plane are affected substantially because of the allowed mixing with *σ*-type orbitals of the same symmetry. Ten of them (the σ-type $2b_u$ and $2a_g$ FMOs, the σ/π-type $1b_u$ and $1a_g$ FMOs, the π-type $1a_u$ and $1b_g$ FMOs, the σ/π*-type $3b_u$ and $3a_g$ FMOs, and the π*-type $2a_u$ and $2b_g$ FMOs) that may be involved in interaction with the metallic fragment are shown on the right-hand side of Fig. 5. They are equally localised overall on C(1) and C(2) atoms.

The pertinent bonding interactions between the metallic fragments and the tetracarbon unit are illustrated in Fig. 5. The six vacant high-lying metallic FMOs ($2a_u$, $3a_g$, $3b_u$, $2b_g$, $4a_g$ and $4b_u$) interact rather strongly with the six occupied low-lying C_4 FMOs, $1b_u$, $1a_u$, $2b_u$, $1a_g$, $1b_g$ and $2a_g$ (see their electron occupation after interaction in Fig. 5). These six bonding interactions mainly account for the ten metal–carbon bonding contacts and reflect the delocalised covalent bonding between the metal framework and the C_4 linkage. At first sight the six lowest FMOs of the metallic fragment, extending mainly in the metal planes, interact poorly with the C_4 chain and remain almost unperturbed after interaction. All are occupied for the observed count of 96 c.v.e., and are mainly responsible for the six metal–metal bonding contacts in molecule **9**. Nevertheless, four of them ($1a_u$, $1b_g$, $2a_g$ and $2b_u$) interact notably with the accepting

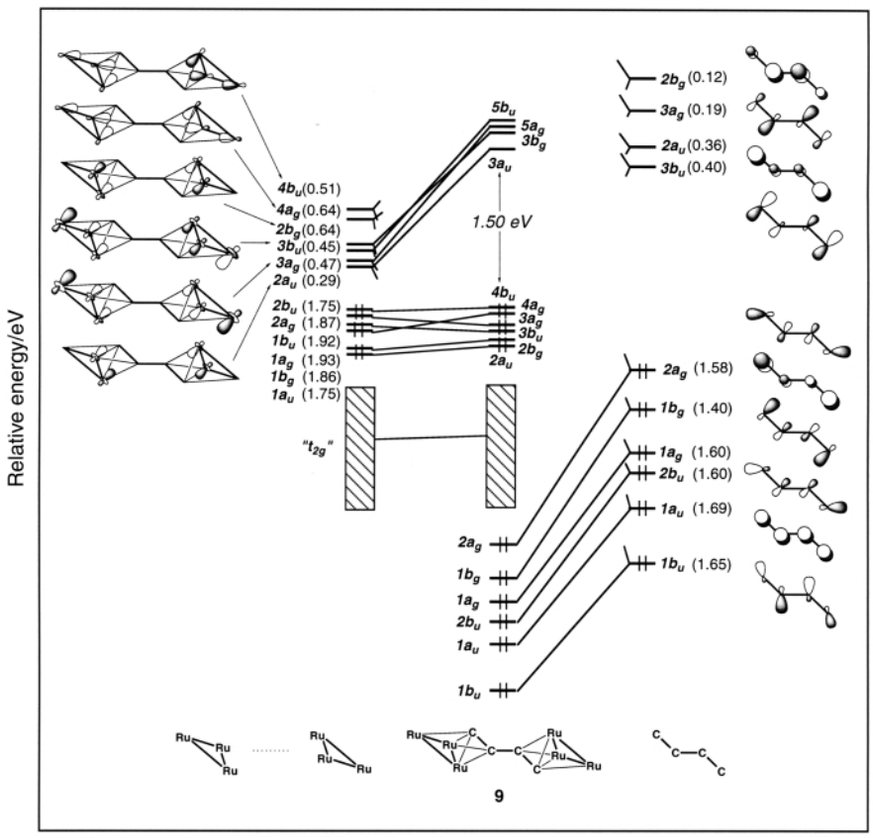

Fig. 5 Qualitative MO diagram based on EH calculations for model **9** obtained from the interaction of the $\{(CO)_9Ru_3 \cdots Ru_3(CO)_9\}$ fragment with the $(C_4)^{2-}$ linkage. The low-lying FMO set of the metallic fragment is not drawn. Symmetry labels are given in C_{2h}. The numbers in brackets indicate the electron occupation of FMOs after interaction.

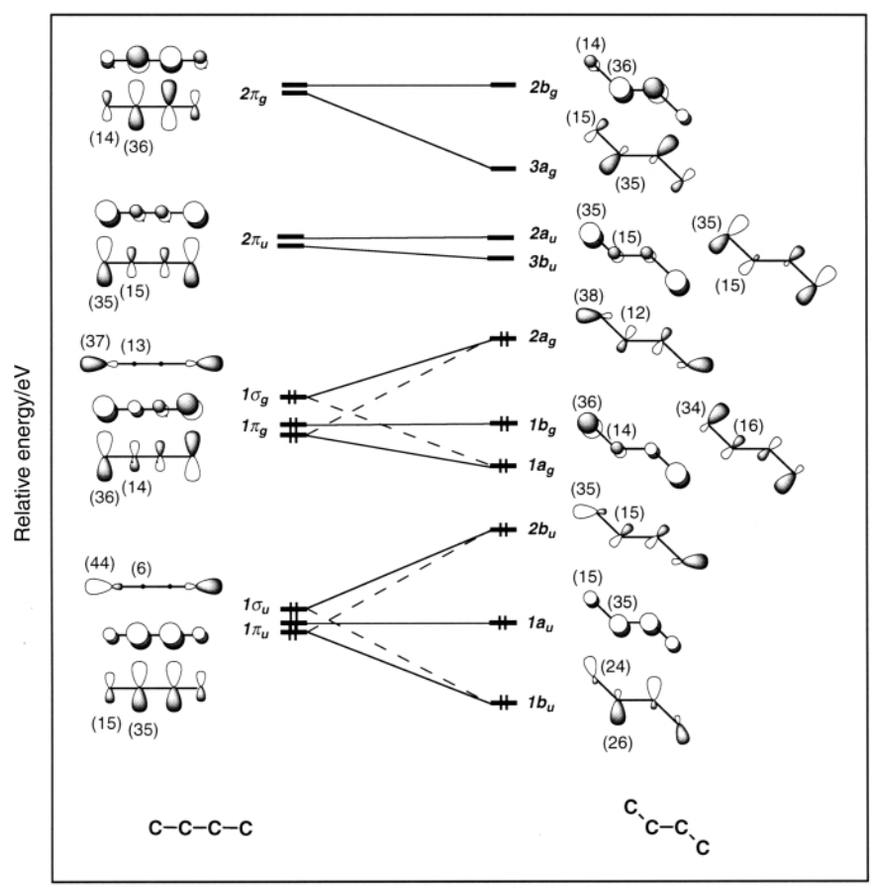

Fig. 6 The frontier orbitals of the linear (left) and bent (right) $(C_4)^{2-}$ group. The numbers indicate the percentage of carbon character.

FMOs of the C_4 unit, $3b_u$, $2a_u$, $3a_g$ and $2b_g$. This electron back donation from the metal fragment towards the C_4 group complements the forward donation from the C_4 unit towards the metal triangles and reinforces the metal–carbon bonding. A substantial HOMO/LUMO gap is computed between the occupied M–M bonding MOs and the vacant M–C antibonding MOs for the count of 96 (2 × 48) c.v.e. This HOMO/LUMO gap is not as large as that computed for diynyl clusters such as $\{Co_3(CO)_9\}_2(\mu_3\text{-}\eta^1:\mu_3\text{-}\eta^1\text{-}CC{\equiv}CC)$.[9] In contrast to the latter, some vacant high-lying metallic FMOs which interact rather strongly with occupied low-lying C_4 FMOs also interact to a lesser extent with the high-lying acceptor C_4 FMOs of the same symmetry (see Fig. 5). These "three-orbital pattern" interactions prevent the metallic FMOs from being highly destabilised in energy. Destabilising mixing with the low-lying occupied C_4 FMOs and stabilising mixing with the high-lying vacant C_4 FMOs renders the resulting LUMOs rather metallic in character and poorly localised on the C_4 chain. This contrasts to the $(\mu_3\text{-}\eta^1:\mu_3\text{-}\eta^1)$-diynyl clusters for which a substantial participation of the C_4 linkage was present in the LUMOs.[9]

EH calculations were carried out on the *cis*-isomeric form of model **9** (see **10**). Surprisingly, although this structural arrangement has not been observed yet, computations indicate that both *trans* and *cis* isomers are nearly isoenergetic. Consequently, the *trans* orientation observed in the crystal for compound **6** may result from crystal lattice effects.

It is expected that replacement of an $Ru(CO)_3$ group by the isolobal $W(CO)_2Cp$ fragment would affect very slightly the qualitative electronic properties of such M_6C_4 complexes. Indeed, tiny differences are computed between model **9** and compound **6** in which an $Ru(CO)_3$ unit has been replaced by a $W(CO)_2Cp$ group in one metal triangle and a bridging hydrogen atom has been added on a metal–metal vector of the other metal triangle (see above). For comparison, EH calculations were also carried out on compounds **4** and **8** as well as on model **11** (isoelectronic and isostructural with **4**), in which the $W(CO)_3Cp$ group was replaced by H. Some EH computed characteristics for these different clusters are summarised in Table 4.

As often computed in all-carbon ligand-containing metal clusters,[9,27] the C_4 unit enters into a synergic bonding interaction with the metal triangles. Starting formally from a $(C_4)^{2-}$ fragment,[26] important electron donation occurs primarily from the occupied low-lying orbitals of the carbon linkage to empty metallic molecular orbitals. This is supplemented by back donation from filled metallic molecular orbitals to the high-lying π* orbitals of the $(C_4)^{2-}$ moiety (see Fig. 6). Forward electron donation is rather similar for model **9** and compound **6** (2.48 *vs.* 2.43 electrons for **9** and **6**, respectively). On the other hand back donation is more important for **6** (1.07 *vs.* 1.36 electrons for **9** and **6**, respectively). Indeed, the presence of one $W(CO)_2Cp$ group in the metal fragment of **6** modifies substantially the extent of localisation and energy of the metallic FMOs. In particular, one of the donor orbitals is heavily weighted towards the tungsten atom and destabilised in energy with respect to those of the donor FMOs of the Ru_6 fragment of **9**. Therefore, this changes the magnitude of the interactions between metallic donor orbitals and C_4 acceptor orbitals which are stronger in **6** than in **9**. Consequently the C_4 bridge is more negatively charged in **6** than in **9** (−0.75 *vs.* −0.46, respectively). The computed net charges on the carbon atoms indicate that the increase of electron density for the C_4 group in **6** with respect to **9** is mainly localised on C(4) bound to W and hardly affects the electronic charge of the other C atoms of the C_4 linkage (compare the atomic net charges of the C atoms for **6** and **9** in Table 4). This might reflect the lack of electronic "communication" between the two metallic moieties through the C_4 bridge in **6**. This statement is supported by computations carried out on compound **4** and model **11** for which the net charges of the two carbon atoms tethered to the Ru_3 triangle are nearly identical to those computed for C(1) and C(2) in **6** and **9**.

An examination of the metal–carbon overlap populations (OP) given in Table 4 indicates that in both compounds **6** and **9** the end carbon atoms C(1) and C(4) are strongly σ ligated to one metal atom (strong OP: *ca.* 0.70) and π bonded to two metal atoms (OP: *ca.* 0.18), whereas the "inner" carbon atoms, C(2) and C(3), are strongly π bonded to two metal atoms (medium OP: *ca.* 0.20). Identical metal-to-carbon bonding is computed for compound **4** and model **11** (see Table 4).

Compound **8** can conceptually be derived from **6** by substituting one RuH group by one Co atom on one triangle and one Ru by Co on the other. This gives $CoRu_2$ and CoRuW cluster units (see above). In the former, the change of Ru by Co accompanied by the "loss" of the bridging hydrogen does not affect the electron count, and a 48-c.v.e. trimetallic acetylide $CoRu_2C_2$ unit is kept. On the other hand, the replacement of Ru by Co brings one more electron to the cluster which forces a rearrangement of the $CoRuWC_2$ core, leading to a 48-c.v.e. trimetallic vinylidene cluster unit. As often found in other cluster-bonded vinylidenes,[22] the alkynylvinylidene cap in **8** bends toward the more electron-poor Ru(6) metal atom. This allows us to assign a formal 18-electron configuration to each of the three metal centers of the triangular cluster unit.[26,28] Indeed, EH calculations carried out on compound **8** indicate a quite substantial Ru(6)-C(3) OP (0.192) comparable to that computed between Ru(6) and the π-ligated C(4) atom (0.209). A large energy gap (1.66 eV) separates the HOMO from the LUMO, ensuring the stability of compound **8** for the observed electron count. Here again the HOMO and LUMO are preponderantly metallic in character with the HOMO rather localised on the CoRuW triangle (in particular on W) and the LUMO rather localised on the $CoRu_2$ triangle.

Discussion

The chemistry described above shows that the diynyl ligand present in complex **1** can act as a normal terminal alkyne in its reactions with $Ru_3(CO)_{12}$ and related complexes, forming first the μ_3-alkyne complexes which are then easily transformed thermally into the corresponding hydrido-alkynyl complexes. The dppm derivative **5** is fluxional in solution, showing similar behaviour to that observed previously with $Ru_3(\mu\text{-}H)(\mu_3\text{-}C_2Bu^t)(\mu\text{-}dppm)(CO)_7$.[17] The crystal structure shows that the C≡C[W(CO)$_3$Cp] moiety is trapped between the phenyl groups of the dppm ligand, so providing a degree of stability to this conformer. However, the NMR spectrum also shows the presence of another conformer which is present in smaller amount, to which is assigned the structure **5b** shown in Scheme 2 because of the equivalence of the two P. We have described the diynyl complex $Ru_3(\mu\text{-}H)(\mu_3\text{-}C_2C{\equiv}CSiMe_3)(\mu\text{-}dppm)(CO)_7$ which has a similar structure.[18] All isomers of **5** interconvert rapidly on the NMR timescale above 333 K.

As discussed earlier, incorporation of a second diynyltungsten fragment occurs in the formation of complex **3** from **2**. In this case it appears to be the non-co-ordinated C≡C triple bond of **2** which cycloadds to the second molecule of **1** and a CO molecule. This is unusual, because addition of the second alkyne or diyne molecule in previously observed reactions occurs by incorporation of the cluster-co-ordinated C≡C triple bond. A recent example is the formation of $Ru_3\{\mu_3\text{-}CPhCC(O)C(SiMe_3)C(C{\equiv}CSiMe_3)CCPh\}(\mu\text{-}dppm)(\mu\text{-}CO)(CO)_6$ in the reaction of $Ru_3(\mu_3\text{-}PhC_2C{\equiv}CPh)(\mu\text{-}dppm)(\mu\text{-}CO)(CO)_7$ with $SiMe_3C{\equiv}CC{\equiv}CSiMe_3$. Here also, reorganisation of the ligands, incorporation of CO and opening of the original triangular Ru_3 core have occurred.[29]

Attempts to incorporate the remaining C≡C triple bond into larger clusters by reactions with iron, ruthenium or cobalt carbonyls gave instead complexes in which the two C_2 fragments act independently, being incorporated into two C_2M_3

Table 4 EH computed characteristics for different M_6C_4 clusters

	4	**6**	**8**	**9**	**11**
Binding energy[a]/eV					
	−9.85	−10.48		−8.99	−14.36
HOMO/LUMO gap/eV					
	1.54	1.73 (2.36)[b]	1.66	1.50 (2.37)[b]	1.96
Atomic net charges					
M(1)	−0.294	−0.408	−0.075	−0.176	−0.288
M(2)	−0.010	−0.046	−0.128	−0.163	0.008
M(3)	−0.010	−0.082	0.060	−0.163	0.008
M(4)	1.105 (W)	1.329 (W)	1.249	−0.176	0.113 (H)
M(5)		−0.407	−0.091	−0.163	
M(6)		−0.289	−0.135	−0.163	
C(1)	−0.275	−0.290	−0.281	−0.280	−0.247
C(2)	0.037	−0.025	0.019	0.050	0.025
C(3)	−0.160	−0.026	−0.074	0.050	0.042
C(4)	−0.422	−0.410	−0.363	−0.280	−0.258
[C_4]	−0.820	−0.751	−0.699	−0.460	−0.435
C_4 FMO occupations					
$1b_u$ (π)	1.69	1.63		1.65	1.67
$1a_u$ (σ_{nb})	1.89	1.68		1.69	1.88
$2b_u$ (π)	1.72	1.62		1.60	1.62
$1a_g$ (σ_{nb})	1.66	1.60		1.60	1.69
$1b_g$ (π_{nb})	1.61	1.42		1.40	1.65
$2a_g$ (σ_{nb})	1.58	1.62		1.58	1.49
$3b_u$ (π_{nb})	0.34	0.50		0.40	0.30
$2a_u$ (σ_{nb})	0.31	0.42		0.36	0.27
$3a_g$ (σ_{nb})	0.08	0.27		0.19	0.05
$2b_g$ (π^*)	0.08	0.17		0.12	0.03
Overlap populations					
M(1)–M(2)	0.173	0.172	0.170	0.165	0.173
M(1)–M(3)	0.173	0.168	0.129	0.165	0.173
M(2)–M(3)	0.058	0.060	0.185	0.196	0.060
M(4)–M(5)		0.146	0.109	0.165	
M(4)–M(6)		0.117	0.130	0.165	
M(5)–M(6)		0.204	0.072	0.196	
M(1)–C(1)	0.698	0.699	0.662	0.648	0.702
M(2)–C(1)	0.187	0.182	0.200	0.188	0.185
M(3)–C(1)	0.187	0.184	0.212	0.188	0.185
M(2)–C(2)	0.202	0.211	0.230	0.190	0.205
M(3)–C(2)	0.202	0.216	0.171	0.190	0.205
M(4)–C(4)	0.528	0.781	0.702	0.648	0.777 (C-H)
M(5)–C(4)		0.178	0.470	0.188	
M(6)–C(4)		0.198	0.209	0.188	
M(5)–C(3)		0.246		0.190	
M(6)–C(3)		0.196	0.192	0.190	
C(1)–C(2)	1.314	1.345	1.375	1.348	1.318
C(2)–C(3)	1.020	0.974	0.888	1.046	1.012
C(3)–C(4)	1.810	1.301	1.029	1.348	1.847

[a] BE = E(complex) − [*E*(metal fragment) + *D*((C_4)$^{2-}$ fragment)]. [b] DF HOMO/LUMO gap in brackets.

clusters which are linked by a C–C single bond. These clusters incorporate the σ-bonded tungsten atom to form an interesting series of mixed-metal cores: with iron or cobalt carbonyls some disorder is found in specific positions. The Group 8 metals react to give bis(μ_3-alkynyl) clusters, the cluster-bound hydride being retained on the cluster which does not incorporate the tungsten. In the product obtained from the reaction with cobalt carbonyl, on the other hand, this hydrogen migrates to the C_4 ligand to give a vinylidene co-ordinated to the CoRuW cluster. It is interesting to recall the reactions of $Co_2Ru(CO)_{11}$ with terminal alkynes, which proceed initially to form hydrido-alkynyl complexes, which then isomerise on warming to give the corresponding vinylidene complexes.[23] Also of interest in this regard is the recent report of the formation of the vinylidene cluster $Co_2Fe\{\mu_3\text{-}C{=}CHC_2H[Co_2(CO)_8]\}(CO)_9$ by heating $Co_2Fe_2\{\mu_3\text{-}C_2C_2H[Co_2(CO)_6]\}(\mu\text{-}CO)_2(CO)_8Cp^*$, one of the products obtained from successive reactions of $Fe(C{\equiv}CC{\equiv}CH)(CO)_2Cp^*$ with $Co_2(CO)_8$ and $Fe_2(CO)_9$.[30]

The precise mechanisms of metal exchange reactions involving metal clusters are still matters of controversy.[31] It is interesting to speculate on the origins of the disorderly incorporation of the iron or cobalt atoms into the clusters found in complexes **7** and **8**. Our previous study of the reactions of $Ru_3(\mu_3\text{-}PhC_2C{\equiv}CPh)(\mu\text{-}CO)(CO)_9$ with $Co_2(CO)_8$ to give the butterfly cluster $Co_2Ru_3(\mu_5\text{-}PhC_2C_2Ph)(\mu\text{-}CO)_3(CO)_{11}$ was interpreted in terms of insertion of cobalt into one Ru-Ru bond, followed by Co–Co bond cleavage and co-ordination of the second C≡C triple bond.[32] In the present case a reasonable interpretation of the formation of products **7** involves addition/exchange of iron with one ruthenium in the Ru_3 cluster; in the course of this reaction only the metal atom σ bonded to the alkynyl fragment is exchanged (but this may be a result of migration of the alkynyl group around the cluster). Elimination and/or co-ordination of FeRu or Ru_2 fragments to the free C≡C triple bond with concomitant addition to the W occurs to give FeRuW or Ru_2W cores.

Table 5 Crystal data and refinement details for complexes **4**–**8**

	4	**5**	**6**	**7a(i)**	**7a(ii)**	**7b(i)**	**7b(ii)**	**8**
Instrument	CCD	Single counter	Single counter	Single counter	CCD	CCD	CCD	Single counter
T/K	*ca.* 153	*ca.* 295	*ca.* 295	*ca.* 295	*ca.* 300	*ca.* 300	*ca.* 300	*ca.* 295
Formula	$C_{21}H_6O_{12}Ru_3W$	$C_{44}H_{28}O_{10}P_2Ru_3W$	$C_{26}H_6O_{17}Ru_3W$	$C_{26}H_6FeO_{17}Ru_4W$		$C_{26}H_6Fe_2O_{17}Ru_3W$		$C_{26}H_6Co_2O_{17}Ru_3W$
M	937.3	1265.7	1279.5	1234.3		1189.1		1195.3
Crystal system	Triclinic	Monoclinic	Monoclinic	Monoclinic		Monoclinic		Triclinic
Space group	$P\bar{1}$	$P2_1/n$	$P2_1/n$	$P2_1/n$		$P2_1/n$		$P\bar{1}$
a/Å	10.029(2)	16.066(13)	8.550(3)	8.499(2)	8.502(2)	8.442(2)	8.464(1)	21.830(11)
b/Å	11.176(2)	15.250(11)	24.014(10)	23.949(11)	23.999(3)	23.940(5)	23.850(3)	9.293(4)
c/Å	12.909(2)	18.269(23)	16.669(6)	16.537(8)	16.551(3)	16.422(3)	16.454(2)	8.991(5)
α/°	105.327(2)							111.73(4)
β/°	108.389(2)	95.15(8)	90.34(3)	90.76(3)	90.778(2)	90.941(5)	90.798(2)	98.27(4)
γ/°	99.929(2)							97.96(4)
V/Å^3	1271	4458	3422	3366	3376	3318	3325	1640
Z	2	4	4	4	4	4	4	2
T (min, max)	0.55, 0.83	0.14, 0.35	0.51, 0.64	Not recorded	0.62, 0.86	0.59, 0.83	0.58, 0.91	0.16, 0.49
μ/cm^{-1}	63	37	56	57	56	57	57	59
N_{total}	14859			12119	35896	36381	38658	11483
N (R_{int})	6256 (0.033)	10241	6008	4233 (0.082)	8561 (0.023)	8324 (0.032)	8349 (0.039)	5744 (0.052)
N_o	5642	7507	3957	1849	6935	5403	6229	4599
R	0.034	0.046	0.034	0.043	0.025	0.039	0.036	0.042
R_w	0.041	0.049	0.034	0.047	0.031	0.042	0.040	0.042

We note that consistent Fe/Ru fractionation is not found in the various samples of complex **7**, even when essentially similar reaction conditions are used. This could indicate that varying degrees of equilibration take place in solution or upon separation by tlc. The bands were not completely resolved on the plates and there may be a continuum of exchanged products, with the more iron-rich products having the lower R_f values.

Conclusion

We have shown further the tendency of the two triple bonds in 1,3-diynes to act independently in their reactions with metal-containing substrates. Products from the reactions described above either retain an uncomplexed C≡C triple bond in the products, or incorporate it into a second, independent metal cluster complex. The two resulting cluster moieties are linked by a C–C single bond.

Stable, closed-shell electronic structures with substantial HOMO/LUMO gaps (see Table 4) are calculated for all the computed complexes and models. Such species should not be very reactive. Nevertheless, with "inner" carbon atoms nearly neutral and "outer" carbon atoms negatively charged, we expect the latter to be rather nucleophilic if the chemical reactions which may occur are charge controlled and affect the C_4 linkage. On the other hand, if the reactions are orbital controlled they should affect the metal triangles since the HOMOs and LUMOs are mainly metallic in character (see above). This contrasts with diynyl clusters such as $\{Co_2M(CO)_8Cp\}(\mu_3\text{-}\eta^1\text{:}\mu_3\text{-}\eta^1\text{-}CC{\equiv}CC)\{Co_2M'(CO)_8Cp\}$ (M = M′ Mo or W; M = Mo, M′ = W), for which a substantial participation of the C_4 linkage was present in both HOMOs and LUMOs.[9]

With LUMOs mainly metallic in character, formal addition of electrons to the $(\mu_3\text{-}\eta^2\text{:}\mu_3\text{-}\eta^2\text{-}C_4)$-containing clusters should lead to opening of the metal triangles as is structurally observed in the 100 (2 × 50) c.v.e. complex $\{M_3(\mu\text{-}PPh_2)(CO)_9\}_2(\mu_3\text{-}\eta^2\text{:}\mu_3\text{-}\eta^2\text{-}C_2C_2)$ (M = Ru or Os).[11]

Of considerable interest is the ability of tungsten diynyl complexes to add further metal–ligand fragments to form clusters and lead to co-ordination of a C≡C triple bond to a metal cluster in either the $\mu_3\text{-}\eta^1$ or the $\mu_3\text{-}\eta^2$ mode, as exemplified in this work. This demonstrates the flexibility of the C_4 ligand which can bind differently to metal clusters in order to satisfy their electronic requirements.

Experimental

General reaction conditions

All reactions were carried out under dry, high purity nitrogen using standard Schlenk techniques. Solvents were dried, distilled and degassed before use. Elemental analyses were by the Canadian Microanalytical Service, Delta, B.C. Preparative TLC was carried out on glass plates (20 × 20 cm) coated with silica gel (Merck 60 GF_{254}, 0.5 mm thick).

Instrumentation

IR: Perkin-Elmer 1700X FT-IR; 683 double beam, NaCl optics. NMR: Gemini 200 (^{1}H at 199.975 MHz, ^{13}C at 50.289 MHz); Bruker ACP300 (^{1}H at 300.13 MHz, ^{13}C at 75.47 MHz). ES mass spectra: samples were dissolved in MeOH and injected directly into a Finnigan LCQ mass spectrometer. Nitrogen was used as the drying and nebulising gas. Chemical aids to ionisation are indicated where required.[33] Analytical and spectroscopic data are collected in Table 1.

Starting materials

$W(C{\equiv}CC{\equiv}CH)(CO)_3Cp$,[1] $Ru_3(CO)_{12}$,[10] $Ru_3(CO)_{10}(NCMe)_2$,[11] $Ru_3(\mu\text{-dppm})(CO)_{10}$[12] and $Fe_2(CO)_9$[13] were made by the cited literature methods. $Co_2(CO)_8$ (Strem) was a fresh sample used as received.

Preparations

$Ru_3\{\mu_3\text{-}HC_2C{\equiv}C[W(CO)_3Cp]\}(\mu\text{-}CO)(CO)_9$ 2. To a solution of $Ru_3(CO)_{10}(NCMe)_2$ [prepared from $Ru_3(CO)_{12}$ (200 mg, 0.312 mmol) in CH_2Cl_2–MeCN (4:1) (100 ml)] was added a solution of $W(C{\equiv}CC{\equiv}CH)(CO)_3Cp$ (240 mg, 0.624 mmol) in CH_2Cl_2 (5 ml). After stirring at r.t. for 30 min the mixture had changed from yellow to dark red. After removal of solvent the residue was dissolved in CH_2Cl_2 and separated by TLC (silica gel, acetone–hexane 3:7). The first yellow band (R_f 0.80) gave $Ru_3(CO)_{12}$ (14 mg, 7%). The second red band (R_f 0.58) gave $Ru_3\{\mu_3\text{-}HC_2C{\equiv}C[W(CO)_3Cp]\}(\mu\text{-}CO)(CO)_9$ **2** (120 mg, 40%) as a dark red powder. Bands 3 and 4 contained small amounts of unidentified materials. Band 5 (R_f 0.50) contained the previously reported complex **3**, obtained as red crystals from CH_2Cl_2–MeOH (20 mg, 5%). This complex could also be synthesized directly from **1** (27 mg, 0.07 mmol) and **2** (70 mg, 0.07 mmol) in thf (10 ml) overnight at r.t. Purification by TLC gave **3** (39 mg, 41%).

$Ru_3(\mu\text{-}H)\{\mu_3\text{-}C_2C{\equiv}C[W(CO)_3Cp]\}(CO)_9$ 4. A solution of complex **2** (130 mg, 0.14 mmol) in benzene (15 ml) was heated at reflux point for 10 min. After evaporation of solvent, purifcation of the residue by TLC (acetone–hexane 3:7) gave a single yellow band (R_f 0.56) from which $Ru_3(\mu\text{-}H)\{\mu_3\text{-}C_2C{\equiv}C[W(CO)_3Cp]\}(CO)_9$ **4** (84 mg, 67%) was isolated as orange crystals (CH_2Cl_2).

$Ru_3(\mu\text{-}H)\{\mu_3\text{-}\eta^1\text{:}\eta^2\text{-}C_2C{\equiv}C[W(CO)_3Cp]\}(\mu\text{-dppm})(CO)_7$ 5. A solution of $W(C{\equiv}CC{\equiv}CH)(CO)_3Cp$ (60 mg, 0.15 mmol) and $Ru_3(\mu\text{-dppm})(CO)_{10}$ (100 mg, 0.10 mmol) in thf (15 ml) was heated at reflux point for 3h in the dark. Preparative TLC (hexane–acetone 75:40) and crystallisation (CH_2Cl_2–MeOH) of the bright yellow band (R_f 0.6) yielded $Ru_3(\mu\text{-}H)\{\mu_3\text{-}\eta^1\text{:}\eta^2\text{-}C_2C{\equiv}C[W(CO)_3Cp]\}(\mu\text{-dppm})(CO)_7$ **5** (120 mg, 92%).

$\{Ru_3(\mu\text{-}H)(CO)_9\}(\mu_3\text{:}\mu_3\text{-}C_2C_2)\{Ru_2W(CO)_8Cp\}$ 6. A mixture of $Ru_3(CO)_{12}$ (32 mg, 0.05 mmol) and complex **4** (50 mg, 0.05 mmol) was heated in refluxing toluene (20 ml) for 30 min. The residue after removal of solvent was purified by TLC (acetone–hexane 3:7) to give recovered $Ru_3(CO)_{12}$ (1.2 mg, 3.8%) from a yellow band (R_f 0.82). The second yellow band (R_f 0.57) afforded yellow-orange crystals (CH_2Cl_2) of $\{Ru_3(\mu\text{-}H)(CO)_9\}(\mu_3\text{:}\mu_3\text{-}C_2C_2)\{Ru_2W(CO)_8Cp\}$ **6** (36 mg, 53%).

$\{Ru_{3-m}Fe_m(\mu\text{-}H)(CO)_9\}(\mu_3\text{:}\mu_3\text{-}C_2C_2)\{Fe_nRu_{2-n}W(CO)_8Cp\}$ 7. Solid $Fe_2(CO)_9$ (20 mg, 0.06 mmol) was added to a solution of complex **4** (30 mg, 0.03 mmol) in toluene (8 ml) and the mixture heated at reflux point for 15 min. Purification by TLC (acetone–hexane 3:7) gave a red band (R_f *ca.* 0.50) which afforded $\{Ru_{3-m}Fe_m(\mu\text{-}H)(CO)_9\}(\mu_3\text{:}\mu_3\text{-}C_2C_2)\{Fe_nRu_{2-n}W(CO)_8Cp\}$ **7** as an orange-red solid (17.4 mg, 45%). Further purification by TLC (acetone–hexane 3:7, followed by benzene–hexane 1:1) resulted in separation into three closely running bands. The first (yellow, R_f 0.55) gave red-orange crystals of **7a** (8.5 mg) (from C_6H_6). The second orange band (R_f 0.52) gave red crystals of **7b** (from PhMe). The IR ν(CO) and ^{1}H NMR spectra were identical to those obtained for the first product, although a single-crystal structure determination showed a total of two Fe atoms had been incorporated. The third red-brown band (R_f 0.50) afforded small red crystals (3 mg), also having IR ν(CO) and ^{1}H NMR spectra identical to those of the other two complexes. Elemental analyses were obtained only for fraction **7a**.

$\{CoRu_2(CO)_9(\mu_3\text{-}\eta^2\text{:}\mu_3\text{-}\eta^2\text{-}CCHC_2)\{CoRuW(\mu\text{-}CO)(CO)_7Cp\}$ 8. Solutions of $Co_2(CO)_8$ (34 mg, 0.1 mmol) in toluene (2 ml) and of complex **4** (44 mg, 0.05 mmol) in toluene (8 ml) were mixed and heated at reflux point for 15 min. The residue obtained after removal of solvent was separated by TLC (acetone–hexane 1:4, followed by benzene–hexane 1:1) into several bands. An unidentified red solid (1 mg) with ν(CO) 2076m, 2058vs, 2049s, 2035m, 2015m, 1986 (sh), 1951w (br) and 1864w (br) cm^{-1} was obtained from band 1 (R_f 0.54). Band 2 (R_f 0.52) afforded dark red crystals (CH_2Cl_2) of $\{CoRu_2(CO)_9\}(\mu_3\text{-}\eta^2\text{:}\mu_3\text{-}\eta^2\text{-}CCHC_2)\{CoRuW(CO)_8Cp\}$ **8** (22 mg, 63%).

Structure determinations

Measurements of diffraction data were carried out in two ways, all instruments being fitted with monochromatic Mo-Kα radiation sources ($\lambda = 0.71073$ Å). (a) Using a single counter/four-circle instrument, N unique data were measured, N_o with $I > 3\sigma(I)$ being used in the refinement after analytical absorption correction. (b) Using a Bruker AXS CCD/area detector instrument, N_{total} reflections were measured, merging, after 'empirical' absorption connection (R_{int} quoted) to N unique using the proprietary software SMART/SAINT/SADABS/XPREP, N_o with $F > 4\sigma(F)$ being considered 'observed' and used in the refinement. In all structures anisotropic thermal parameter forms were refined for the non-hydrogen atoms, (x, y, z, $U_{iso})_H$ being included, constrained at estimated values. Conventional residuals, R, R_w (statistical weights) on $|F|$ are quoted at convergence; neutral atom complex scattering factors were employed, as was the XTAL 3.4 program system.[34]

Variata. *Complex* ***4.*** All hydrogen atoms were refined in (x, y, z, U_{iso}).

Complexes ***5a*** *and* ***6.*** A four-circle instrument was used. (x, y, z, U_{iso}) were refinable for the core hydrogen, enhancing its credibility as modelled.

Complex 7. At the start of this work only a single counter diffractometer was available: complex **7a** was amenable to study with this instrument, while **7b** was not. Specimens available from crystallisation of the bands constituting **7a** and **7b** were small, of marginal size, so that **7a** only was amenable to study using a single counter instrument. Although of good quality, data were limited. A sphere was measured to optimise the result, which was modelled in terms of disorder among the metal atoms; individual sites were not resolvable here, nor for the ligand atoms, so that metal atoms were modelled as composite with site occupancies refined as x_{Ru} for the ruthenium component with a complementary $1 - x_{Ru}$ iron component and common thermal parameters, the tungsten seemingly unambiguous. Sites 2 and 3 exhibited negligible iron occupancy and x_{Ru} was set at unity. For sites 1, 5, 6, x_{Ru} were 0.694(8), 0.478(8), 0.860(8), totalling 2.0_3 with the strong implication that the M_6 complement comprises $FeRu_4W$. This result is designated **7a(i)**. With the advent of the CCD facility, **7b** was revisited and now found to be tractable **[7b(i)]**. Again occupancies of sites 1, 5, 6 were modelled as mixed, populations x_{Ru} refining to 0.554(6), 0.083(6), 0.364(6), total 1.0_0, indicative of an Fe_2Ru_3W metal complement, suggesting that during TLC $FeRu_4W$ and Fe_2Ru_3W species travel as separate bands, but that each band may be an unresolved aggregate of isomers. The interest and significance of this result was such that it was desirable to carry out a redetermination of **7a** with the CCD facility. The useful component of the original sample (which comprised only a very few very small crystals) was exhausted, so that a new sample was supplied from a newly synthesized batch. For this determination, **7a(ii)**, x_{Ru}(1,5,6) were found to be 0.740(3), 0.407(3), 0.872(3), total 2.0_2, *the individual components exhibiting significantly different occupancies at sites 1, 5.*

While the precision of the earlier single counter study of complex **7a(i)** falls short of that of the CCD study **7a(ii)**, the care taken in the measurement, together with the magnitude of the s.u.s suggested that a difference of the magnitude observed should be considered seriously. Whence its possible origin? It seems most unlikely that a change of this magnitude could result from differing populations in a fluxional thermal equi-

librium induced by any temperature difference, which must be minor, between the two experiments. Rather, it would seem that the origin lies in the use of two different synthetic batches; these are thermal in origin, and it appeared possible that different equilibria at significantly different elevated temperatures may have resulted in different $FeRu_4W$ isomeric mixes. In the light of this a re-examination of a fresh sample of **7b** was undertaken [original sample **7b(i),** new sample **7b(ii)**], site occupancies of sites 1, 5, 6 now refining to x_{Ru} 0.257(5), 0.183(4), 0.478(4), total 0.92. This result deviates from unity more significantly than the above values and may be a more realistic indicator of appropriate error estimates in the context of the refinement of parameters which are inherently correlated, the totalities rather than the internal relativities being the parameter more likely to be influenced by specimen and experimental vicissitudes dependent on $(\sin\theta)/\lambda$. Nevertheless, it is of interest to observe here also very substantial differences in the proportions of the components for the complexes of the same stoichiometry originating from independent syntheses which, in turn, may be the cause. All hydrogen atoms were located and refined in (x, y, z, U_{iso}) in the **7a(ii)**, **7b** determinations.

Complex ***8.*** Single counter data were employed, a full sphere being measured. Here again the refinement suggested mixed occupancies, here of sites 2,3, x_{Ru} for site 2 refining to 0.859(6), with other populations following from the constraint imposed, after trial refinement, of 1 : 1 Co : Ru stoichiometry over the two sites, overall Co_2Ru_3W. The hydrogen on C(3) was located and refined in (x, y, z, U_{iso}).

CCDC reference number 186/2066.

See http://www.rsc.org/suppdata/dt/b0/b002406f/ for crystallographic files in .cif format.

Theoretical calculations

DF. Density functional calculations were carried out on model **9** and compound **6** using the Amsterdam Density Functional (ADF) program[35] developed by Baerends and coworkers[36] using the local density approximation (LDA) in the Vosko–Wilk–Nusair parametrisation.[37] The atom electronic configurations were described by a double-ξ Slater-type orbital (STO) basis set for H 1s, C 2s and 2p, O 2s and 2p, augmented with a 3d single-ξ polarisation function for the carbon atoms of the C_4 chain. A triple-ξ STO basis set was used for Ru 4d and 5s and for W 5d and 6s, augmented with a single-ξ 5p polarisation function for Ru and augmented with a single-ξ 6p polarisation function for W. A frozen-core approximation was used to treat the core shells up to 1s for C and O, up to 4p for Ru and up to 5p for W.[36a] The geometry of model **9**[27] was optimised using the analytical gradient method implemented by Verluis and Ziegler.[38]

EH. Extended Hückel calculations were carried out within the extended Hückel formalism[39] using the program CACAO.[40] The Slater exponents (ξ) and the valence shell ionisation potentials (H_{ii} in eV) were respectively: 1.3, −13.6 for H 1s; 1.625, −21.4 for C 2s; 1.625, −11.4 for C 2p; 2.275, −32.4 for O 2s; 2.275, −14.8 for O 2p; 2.00, −9.21 for Co 4s; 2.00, −5.29 for Co 4p; 2.078, −8.60 for Ru 5s; 2.043, −5.10 for Ru 5p; 2.341, −8.26 for W 6s; 2.309, −5.17 for W 6p. The H_{ii} value for Co 3d, Ru 4d, and W 5d was at −13.18, −12.20, and −10.37 eV respectively. A linear combination of two Slater-type orbitals with exponents $\xi_1 = 5.55$ and $\xi_2 = 1.90$; $\xi_1 = 5.378$ and $\xi_2 = 2.303$; $\xi_1 = 4.982$ and $\xi_2 = 2.068$ with the weighting coefficients $c_1 = 0.5551$ and $c_2 = 0.6461$; $c_1 = 0.5340$ and $c_2 = 0.6365$; $c_1 = 0.6940$ and $c_2 = 0.5631$ was used to represent the Co 3d, Ru 4d, and W 5d atomic orbitals, respectively. EH calculations were carried out using the DF-optimised geometry of model **9** and the experimental structures of complexes **4**, **6**, and **8**. The geometry of model **10** was derived from compound **4** by replacing the $W(CO)_2Cp$ unit by a hydrogen atom. The C–H distance was set at 1.09 Å.

Acknowledgements

Support of this work by the Australian Research Council (ARC) is gratefully acknowledged. These studies were also greatly facilitated by travel grants (ARC IREX programme and the Centre National de la Recherche Scientifique, France). PJL held an Australian Post-Graduate Research Award. Johnson Matthey Technology plc, Reading, UK, generously loaned the $RuCl_3{\cdot}nH_2O$. SK and J-FH thank the Centre de Ressources Informatiques (CRI) of Rennes and the Institut de Développement et de Ressources en Informatique Scientifique (IDRIS-CNRS) of Orsay for computing facilities. We thank Professor Brian Nicholson (University of Waikato, Hamilton, New Zealand) for some of the electrospray mass spectra.

References

1 P. Belanzoni, N. Re, A. Sgamellotti and C. Floriani, *J. Chem. Soc., Dalton Trans.*, 1998, 1825, and references cited therein.
2 P. Belanzoni, N. Re, M. Rosi, A. Sgamellotti and C. Floriani, *Organometallics*, 1996, **15**, 4264; P. Belanzoni, N. Re, A. Sgamellotti and C. Floriani, *J. Chem. Soc., Dalton Trans.*, 1997, 4773.
3 Y. Zhou, J. W. Seyler, W. Weng, A. M. Arif and J. A. Gladysz, *J. Am. Chem. Soc.*, 1993, **115,** 8509; J. W. Seyler, W. Weng, Y. Zhou and J. A. Gladysz, *Organometallics*, 1993, **12**, 3802.
4 N. Le Narvor and C. Lapinte, *J. Chem. Soc., Chem. Commun.*, 1993, 357; N. Le Narvor, L. Toupet and C. Lapinte, *J. Am. Chem. Soc.*, 1995, **117**, 7129.
5 M. Brady, W. Weng and J. A. Gladysz, *J. Chem. Soc., Chem. Commun.*, 1994, 2655; T. Bartik, B. Bartik, M. Brady, R. Dembinsky and J. A. Gladysz, *Angew. Chem.*, 1996, **108**, 467; *Angew. Chem., Int. Ed. Engl.*, 1996, **35**, 414; B. Bartik, R. Dembinski, T. Bartik, A. M. Arif and J. A. Gladysz, *New J. Chem.*, 1997, **21**, 739.
6 F. Coat and C. Lapinte, *Organometallics*, 1996, **15**, 477.
7 B. H. Robinson and J. L. Spencer, *J. Organomet. Chem.*, 1971, **30**, 267; R. J. Dellaca, B. R. Penfold, B. H. Robinson, W. T. Robinson and J. L. Spencer, *Inorg. Chem.*, 1970, **9**, 2204; R. J. Dellaca and B. R. Penfold, *Inorg. Chem.*, 1971, **10**, 1269.
8 G. H. Worth, B. H. Robinson and J. Simpson, *Organometallics*, 1992, **11**, 3863.
9 M. I. Bruce, J.-F. Halet, S. Kahlal, P. J. Low, B. W. Skelton and A. H. White, *J. Organomet. Chem.*, 1999, **578**, 155.
10 D. M. Norton, C. L. Stern and D. F. Shriver, *Inorg. Chem.*, 1994, **33**, 2701.
11 C. J. Adams, M. I. Bruce, E. Horn, B. W. Skelton, E. R. T. Tiekink and A. H. White, *J. Chem. Soc., Dalton Trans.*, 1993, 3299.
12 S. B. Falloon, A. M. Arif and J. A. Gladysz, *Chem. Commun.*, 1997, 629; S. B. Falloon, S. Szafert, A. M. Arif and J. A. Gladysz, *Chem. Eur. J.*, 1998, **4**, 1033.
13 M. I. Bruce, M. Ke, P. J. Low, B. W. Skelton and A. H. White, *Organometallics*, 1998, **17**, 3539.
14 M. I. Bruce, B. W. Skelton, A. H. White and N. N. Zaitseva, *J. Chem. Soc., Dalton Trans.*, 1996, 3151.
15 M. I. Bruce, P. A. Humphrey, E. Horn, E. R. T. Tiekink, B. W. Skelton and A. H. White, *J. Organomet. Chem.*, 1992, **429**, 207.
16 M. I. Bruce, N. N. Zaitseva, B. W. Skelton and A. H. White, *J. Organomet. Chem.*, 1997, **536–537**, 93.
17 G. Predieri, A. Tiripicchio, C. Vignali and E. Sappa, *J. Organomet. Chem.*, 1988, **342**, C33.
18 M. I. Bruce, P. J. Low, A. Werth, B. W. Skelton and A. H. White, *J. Chem. Soc., Dalton Trans.*, 1996, 1551.
19 V. A. Semion and Yu. T. Struchkov, *Zh. Strukt. Khim.*, 1968, **9**, 1046; M.-C. Chen, Y.-J. Tsai, C.-T. Chen, Y.-C. Lin, T.-W. Tseng, G.-H. Lee and Y. Wang, *Organometallics*, 1991, **10**, 378.
20 D. Braga, L. J. Farrugia, A. L. Gillon, F. Grepioni and E. Tedesco, *Organometallics*, 1996, **15**, 4684.
21 M. I. Bruce, N. N. Zaitseva, B. W. Skelton and A. H. White, *J. Cluster Sci.*, 1996, **7**, 109.
22 M. I. Bruce, *Chem. Rev.*, 1991, **91**, 197 and references therein.
23 E. Roland, W. Bernhardt and H. Vahrenkamp, *Chem. Ber.*, 1985, **118**, 2858.
24 Model **9** was optimized with the aid of DF calculations under the C_{2h} symmetry constraint in order to reduce computational effort. The following distances (Å) and bond angles (°) were obtained: Ru(1)–Ru(2–3) 2.794; Ru(2)–Ru(3) 2.750; Ru(1)–C(1) 1.993; Ru(2,3)–C(1) 2.220; Ru(2,3)–C(2) 2.245; C(1)–C(2) 1.314; C(2)–C(3) 1.374; Ru–C(O) (av.) 1.913; C–O (av.) 1.178; C(1)–C(2)–C(3) 152.5. A HOMO/LUMO gap of 2.47 eV was computed.

25 There are different ways to count electrons formally in the tetracarbon moiety. We choose here to consider C_4 as a dianionic species rather than a neutral species in order that it agrees with the octet rule. Note that the number of frontier molecular orbitals of C_4 which may participate to the M–C bonding is independent of the electron-counting convention.
26 B. E. R. Schilling and R. Hoffmann, *J. Am. Chem. Soc.*, 1979, **101**, 3456.
27 J.-F. Halet and D. M. P. Mingos, *Organometallics*, 1988, **7**, 51; G. Frapper and J.-F. Halet, *Organometallics*, 1995, **14**, 5044; G. Frapper, J.-F. Halet and M. I. Bruce, *Organometallics*, 1997, **16**, 2590.
28 M. J. McGlinchey, in *Topics in Physical Organometallic Chemistry*, ed. M. Gielen, Freund Publishing House, London, 1992, vol. 4, p. 41.
29 M. I. Bruce, N. N. Zaitseva, B. W. Skelton and A. H. White, *Izv. Akad. Nauk*, *Ser. Khim.*, 1998, 1012; *Russ. Chem. Bull.*, 1998, **47**, 983.
30 M.-C. Chung, A. Sakurai, M. Akita and Y. Moro-oka, *Organometallics*, 1999, **18**, 4684.
31 H. Vahrenkamp, *Adv. Organomet. Chem.*, 1983, **22**, 169; R. D. Adams, in *Comprehensive Organometallic Chemistry II*, eds. E. W. Abel, F. G. A. Stone and G. Wilkinson, Pergamon, Oxford, 1995, vol. 1, ch. 1, pp. 1–22.
32 M. I. Bruce, N. N. Zaitseva, B. W. Skelton and A. H. White, *Polyhedron*, 1995, **14**, 2647.
33 W. Henderson, J. S. McIndoe, B. K. Nicholson and P. J. Dyson, *J. Chem. Soc.*, *Dalton Trans.*, 1998, 519.
34 S. R. Hall, G. S. D. King and J. M. Stewart (Editors), *The XTAL 3.4 Users' Manual*, University of Western Australia, Lamb, Perth, 1994.
35 Amsterdam Density Functional (ADF) Program, release 2.0.1, Vrije Universteit, Amsterdam, 1996.
36 (*a*) E. J. Baerends, D. E. Ellis and P. Ros, *Chem. Phys.*, 1973, **2**, 41; (*b*) E. J. Baerends and P. Ros, *Int. J. Quantum Chem.*, 1978, **S12**, 169; (*c*) P. M. Boerrigter, G. te Velde and E. J. Baerends, *Int. J. Quantum Chem.*, 1988, **33**, 87; (*d*) G. te Velde and E. J. Baerends, *J. Comput. Phys.*, 1992, **99**, 84.
37 S. D. Vosko, L. Wilk and M. Nusair, *Can. J. Chem.*, 1990, **58**, 1200.
38 L. Verluis and T. Ziegler, *J. Chem. Phys.*, 1988, **322**, 88.
39 R. Hoffmann, *J. Chem. Phys.*, 1963, **39**, 1397; R. Hoffmann and W. N. Lipscomb, *J. Chem. Phys.*, 1962, **36**, 2179.
40 C. Mealli and D. Proserpio, *J. Chem. Educ.*, 1990, **67**, 399.